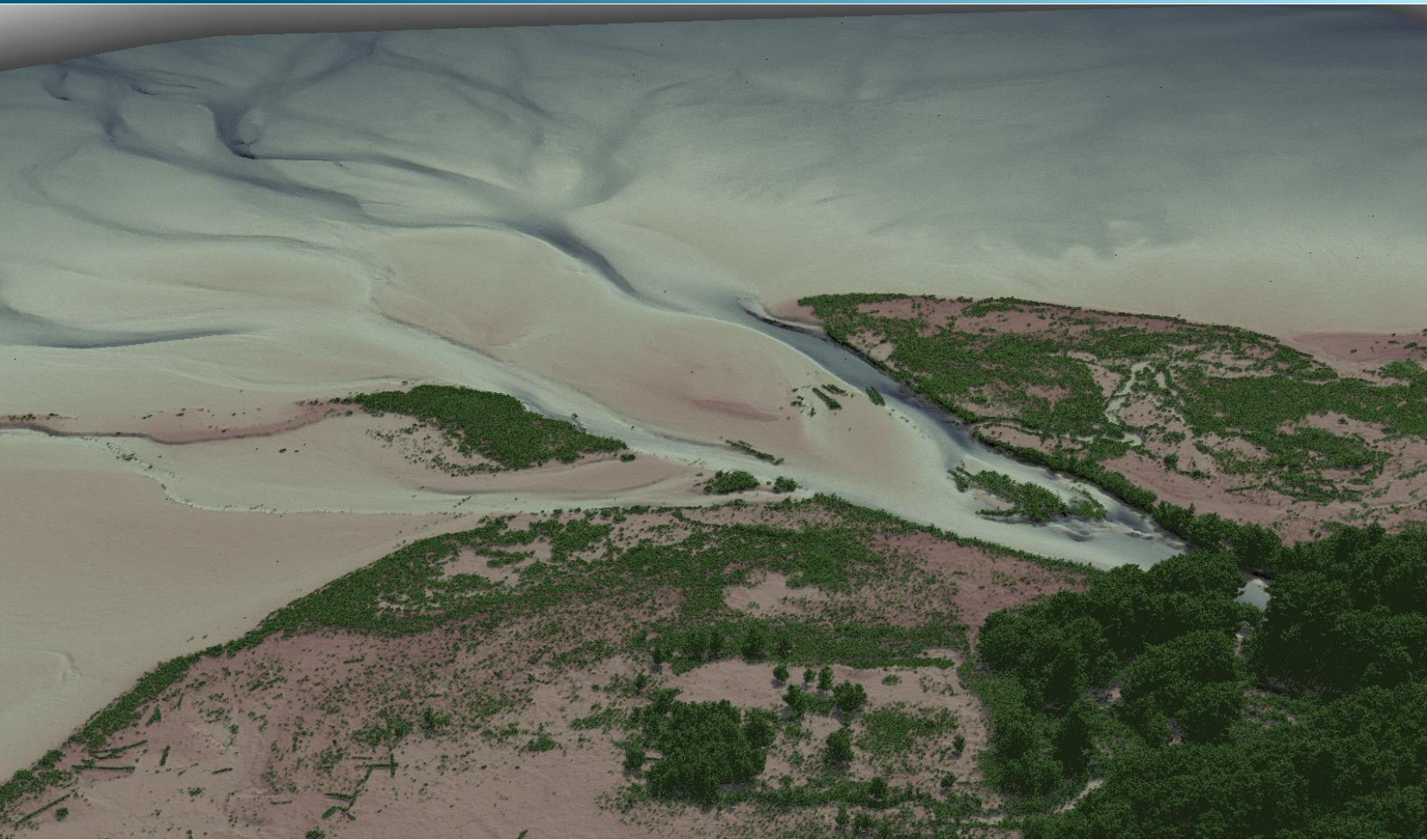


March 14, 2017



# Dungeness, Washington

## Topobathymetric LiDAR Technical Data Report



**Robert Knapp**  
Jamestown S'Klallam Tribe  
1033 Old Blyn Highway  
Sequim, WA 98382  
PH: 360-681-4666



**QSI Corvallis**  
517 SW 2<sup>nd</sup> St., Suite 400  
Corvallis, OR 97333  
PH: 541-752-1204



# TABLE OF CONTENTS

- INTRODUCTION ..... 1
  - Deliverable Products ..... 2
- ACQUISITION ..... 4
  - Sensor Selection: the Riegl VQ-820-G ..... 4
  - Planning..... 4
  - Airborne LiDAR Survey ..... 7
  - Ground Control..... 8
    - Monumentation ..... 8
    - Ground Survey Points (GSPs)..... 9
- PROCESSING ..... 12
  - Topobathymetric LiDAR Data ..... 12
  - Bathymetric Refraction ..... 14
  - LiDAR Derived Products..... 14
    - Topobathymetric DEMs..... 14
    - Intensity Images..... 15
- RESULTS & DISCUSSION ..... 16
  - Mapped Bathymetry..... 16
  - LiDAR Point Density ..... 18
    - First Return Point Density..... 18
    - Bathymetric and Ground Classified Point Densities ..... 22
  - LiDAR Accuracy Assessments ..... 24
    - LiDAR Absolute Accuracy ..... 24
    - LiDAR Relative Vertical Accuracy ..... 27
- CERTIFICATIONS ..... 30
- SELECTED IMAGES..... 31
- GLOSSARY ..... 34
- APPENDIX A - ACCURACY CONTROLS ..... 35

**Cover Photo:** A view of the mouth of the Dungeness River meeting the Pacific Ocean. The image is created from the gridded, bare earth and bathymetric LiDAR returns colored by elevation and above ground LiDAR point cloud.





# INTRODUCTION

This photo taken by QSI acquisition staff shows a view of the Dungeness River in Washington State.



In October 2016, Quantum Spatial (QSI) was contracted by the Jamestown S’Klallam Tribe to collect topobathymetric Light Detection and Ranging (LiDAR) data in the winter of 2016 for the Dungeness site in Washington State. The Dungeness, Washington project area covers the Dungeness coastline between Oyster House Road and Glerin Creek, and stretches from the mouth of the Dungeness River inland approximately 10 miles (Figure 1). Traditional near-infrared (NIR) LiDAR was fully integrated with green wavelength return data (bathymetric) LiDAR in order to provide seamless and complete project mapping. Data were collected to aid the Jamestown S’Klallam Tribe in assessing the channel morphology and topobathymetric surface of the study area.

This report accompanies the delivered topobathymetric LiDAR data and documents contract specifications, data acquisition procedures, processing methods, and analysis of the final dataset including LiDAR accuracy and density. Acquisition dates and acreage are shown in Table 1, a complete list of contracted deliverables provided to the Jamestown S’Klallam Tribe is shown in Table 2, and the project extent is shown in Figure 1.

**Table 1: Acquisition dates, acreage, and data types collected on the Dungeness, Washington site**

Project Site	Contracted Acres	Buffered Acres	Acquisition Dates	Data Type
Dungeness, Washington	5,451	6,655	12/14/2016 - 12/16/2016	LiDAR

# Deliverable Products

**Table 2: Products delivered to Jamestown S’Klallam Tribe for the Dungeness, Washington site**

<b>Dungeness, Washington Topobathymetric LiDAR Products</b> <b>Projection: Washington State Plane North FIPS 4601</b> <b>Horizontal Datum: NAD83 (2011)</b> <b>Vertical Datum: NAVD88 (GEOID12B)</b> <b>Units: US Survey Feet</b>	
<b>Topobathymetric LiDAR</b>	
<b>Points</b>	LAS v 1.2 <ul style="list-style-type: none"> <li>All Classified Returns</li> </ul>
<b>Rasters</b>	3.0 Foot ESRI Grids <ul style="list-style-type: none"> <li>Topobathymetric Bare Earth Digital Elevation Model (DEM)</li> <li>Topobathymetric Bare Earth Digital Elevation Model Clipped to Bathymetric Void Shape (DEM)</li> <li>Highest Hit Digital Surface Model (DSM)</li> </ul> 1.5 Foot GeoTiffs <ul style="list-style-type: none"> <li>Green Sensor Intensity Image</li> <li>NIR Sensor Intensity Image</li> </ul>
<b>Vectors</b>	Shapefiles (*.shp) <ul style="list-style-type: none"> <li>Site Boundary</li> <li>LiDAR Tile Index (1500 ft x 1500 ft)</li> <li>Water’s Edge Breaklines</li> <li>Bathymetric Coverage Polygon</li> <li>Ground Survey Points and Monument Locations</li> </ul>



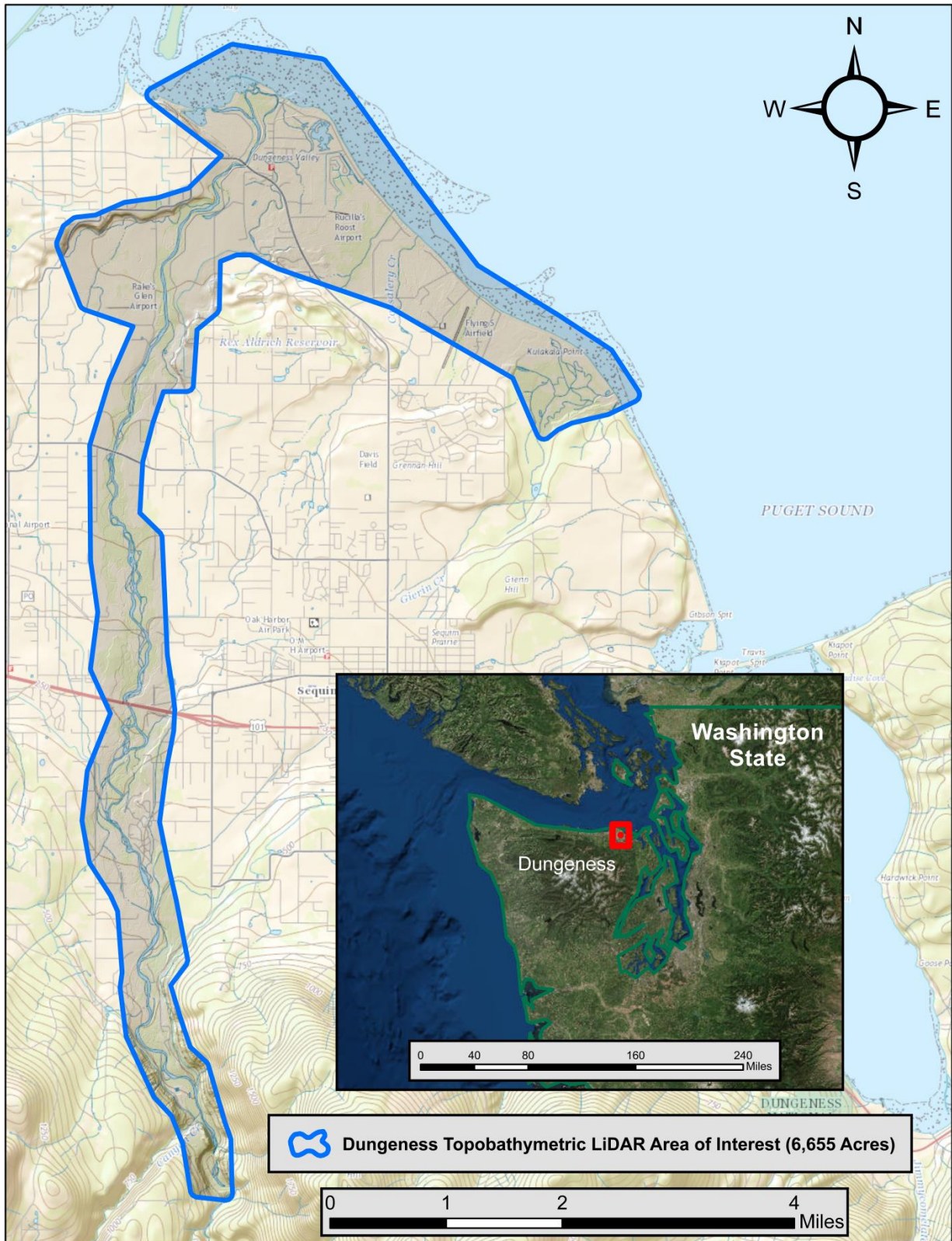


**Figure 1: Location map of the Dungeness Topobathymetric LiDAR site in Washington State**

QSI's Cessna Caravan



## Sensor Selection: the Riegl VQ-820-G

The Riegl VQ-820-G was selected as the hydrographic airborne laser scanner for the Dungeness, Washington Topobathymetric LiDAR project based on fulfillment of several considerations deemed necessary for effective mapping of the project site. A high repetition pulse rate, high scanning speed, small laser footprint, and wide field of view allow for seamless collection of high resolution data of both topographic and bathymetric surfaces. A short laser pulse length allows for discrimination of underwater surface expression in shallow water, critical to shallow and dynamic environments such as the Dungeness River. Sensor specifications and settings for the Dungeness, Washington LiDAR acquisition are displayed in Table 6.

## Planning

In preparation for data collection, QSI reviewed the project area and developed a specialized flight plan to ensure complete coverage of the Dungeness, Washington LiDAR study area at the target point density of  $\geq 4.0$  points/m<sup>2</sup> for green LiDAR returns, and  $\geq 6.0$  points/m<sup>2</sup> for NIR LiDAR returns (determined by the altitude required for flying topo-bathymetry). Acquisition parameters including orientation relative to terrain, flight altitude, pulse rate, scan angle, and ground speed were adapted to optimize flight paths and flight times while meeting all contract specifications.

Factors such as satellite constellation availability and weather windows must be considered during the planning stage. Any weather hazards or conditions affecting the flight were continuously monitored due to their potential impact on the daily success of airborne and ground operations. In addition, logistical considerations including private property access and potential air space restrictions, and channel flow rates (Figure 2 and Figure 3), tidal conditions and water clarity were reviewed.



NOAA/NOS/CO-OPS  
 Daily Tide Prediction for Dungeness,WA  
 StationId 9444471  
 From: 2016/12/14 - 2016/12/15  
 Units: Feet Time Zone: LST/LDT Datum: MLLW

Referenced to Station: Port Townsend ( 9444900 )  
 Time offset in mins (high:-54 low: -38) Height offset in feet (high:\* 0.90 low: \*0.90)

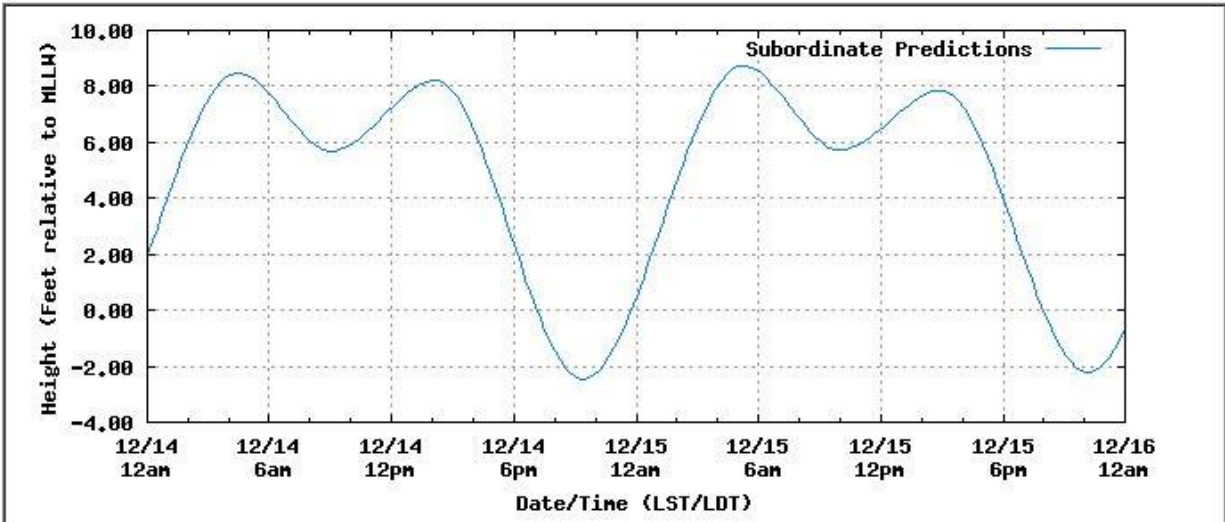


Figure 2: NOAA Station 9444471 tidal gauge height along the Dungeness River at the time of LiDAR acquisition

NOAA/NOS/CO-OPS  
 Daily Tide Prediction for Dungeness,WA  
 StationId 9444471  
 From: 2016/12/15 - 2016/12/16  
 Units: Feet Time Zone: LST/LDT Datum: MLLW

Referenced to Station: Port Townsend ( 9444900 )  
 Time offset in mins (high:-54 low: -38) Height offset in feet (high:\* 0.90 low: \*0.90)

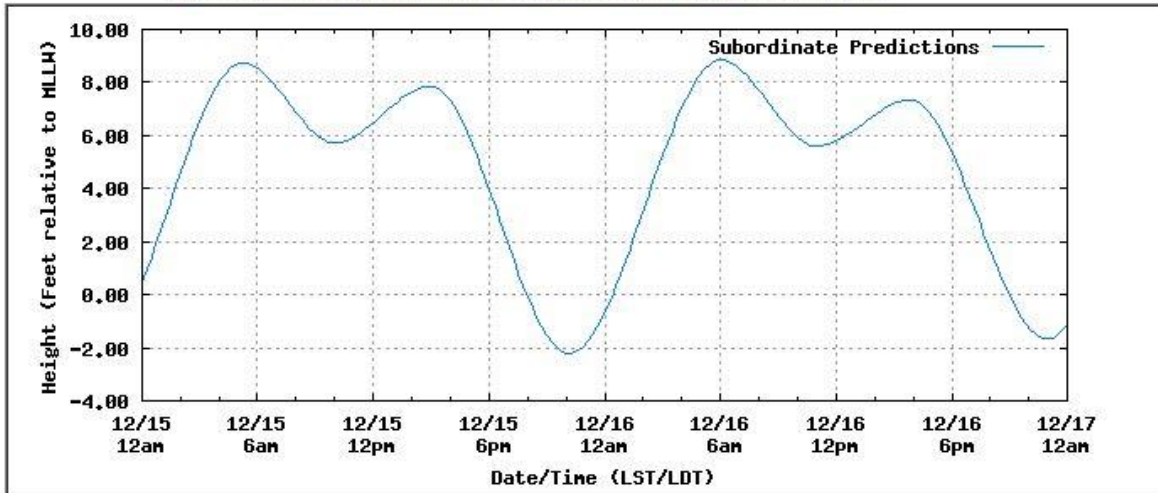


Figure 3: NOAA Station 9444471 tidal gauge height along the Dungeness River at the time of LiDAR acquisition





**Figure 4: Photos taken by QSI acquisition staff which document water clarity of the Dungeness River at the time of LiDAR acquisition**

## Airborne LiDAR Survey

The LiDAR survey was accomplished using a Leica ALS80 system dually mounted with a Riegl VQ-820-G topobathymetric sensor in a Cessna Caravan. The Riegl VQ-820-G uses a green wavelength ( $\lambda=532$  nm) laser that is capable of collecting high resolution vegetation and topography data, as well as penetrating the water surface with minimal spectral absorption by water. The typical number of returns digitized from a single pulse range from 1 to 7 for the Dungeness, Washington topobathymetric LiDAR project area. The Leica ALS80 laser system can record unlimited range measurements (returns) per pulse. It is not uncommon for some types of surfaces (e.g., dense vegetation or water) to return fewer pulses to the LiDAR sensor than the laser originally emitted. The discrepancy between first return and overall delivered density will vary depending on terrain, land cover, and the prevalence of water bodies. All discernible laser returns were processed for the output dataset. Table 3 summarizes the settings used to yield an average pulse density of  $\geq 4.0$  pulses/m<sup>2</sup> for green LiDAR returns and  $\geq 6.0$  pulses/m<sup>2</sup> for NIR LiDAR returns over the Dungeness, Washington topobathymetric LiDAR project area.

**Table 3: LiDAR specifications and survey settings**

LiDAR Survey Settings & Specifications		
<b>Acquisition Dates</b>	December 14 - 16, 2016	December 14 – 16, 2016
<b>Aircraft Used</b>	Cessna Caravan	Cessna Caravan
<b>Sensor</b>	Leica	Riegl
<b>Laser</b>	ALS80	VQ-820G
<b>Maximum Returns</b>	Unlimited	Unlimited
<b>Resolution/Density</b>	Average 6 pulses/m <sup>2</sup>	Average 4 pulses/m <sup>2</sup>
<b>Nominal Pulse Spacing</b>	0.4 m	0.5 m
<b>Survey Altitude (AGL)</b>	450 m, 650 m, 750 m	450 m, 650 m, 750 m
<b>Survey speed</b>	110 knots	110 knots
<b>Field of View</b>	40°	40°
<b>Mirror Scan Rate</b>	51.97 Hz	51.97 Hz
<b>Target Pulse Rate</b>	569 kHz, 404.4 kHz, 353.4 kHz	284 kHz
<b>Pulse Length</b>	2.5 ns	1.2 ns
<b>Laser Pulse Footprint Diameter</b>	9.9 cm, 14.3 cm, 16.5 cm	45 cm, 65 cm, 75 cm
<b>Central Wavelength</b>	1064 nm	532 nm
<b>Pulse Mode</b>	Single Pulse in Air (SPiA)	Single Pulse in Air (SPiA)
<b>Beam Divergence</b>	22 mrad	1 mrad
<b>Swath Width</b>	546 m	546 m
<b>Swath Overlap</b>	60 %	60 %
<b>GPS Baselines</b>	$\leq 13$ nm	$\leq 13$ nm
<b>GPS PDOP</b>	$\leq 3.0$	$\leq 3.0$
<b>GPS Satellite Constellation</b>	$\geq 6$	$\geq 6$
<b>Intensity</b>	8-bit, scaled to 16-bit	16-bit
<b>Accuracy</b>	RMSE <sub>z</sub> $\leq 15$ cm	RMSE <sub>z</sub> $\leq 30$ cm



All areas were surveyed with an opposing flight line side-lap of  $\geq 50\%$  ( $\geq 100\%$  overlap) in order to reduce laser shadowing and increase surface laser painting. To accurately solve for laser point position (geographic coordinates x, y and z), the positional coordinates of the airborne sensor and the attitude of the aircraft were recorded continuously throughout the LiDAR data collection mission. Position of the aircraft was measured twice per second (2 Hz) by an onboard differential GPS unit, and aircraft attitude was measured 200 times per second (200 Hz) as pitch, roll and yaw (heading) from an onboard inertial measurement unit (IMU). To allow for post-processing correction and calibration, aircraft and sensor position and attitude data are indexed by GPS time.

## Ground Control

Ground control surveys, including monumentation and ground survey points (GSPs), were conducted to support the airborne acquisition. Ground control data were used to geospatially correct the aircraft positional coordinate data and to perform quality assurance checks on final LiDAR data.



*QSI-Established Monument*

## Monumentation

The spatial configuration of ground survey monuments provided redundant control within 13 nautical miles of the mission areas for LiDAR flights. Monuments were also used for collection of ground survey points using real time kinematic (RTK) and post processed kinematic (PPK) survey techniques.

Monument locations were selected with consideration for satellite visibility, field crew safety, and optimal location for GSP coverage. QSI established two new monuments for the Dungeness, Washington Topobathymetric LiDAR project (Table 4, Figure 5). New monumentation was set using 5/8" x 30" rebar topped with stamped 2" aluminum caps. QSI's professional land surveyor, Evon Silvia (WAPLS#53957) oversaw and certified the establishment of all monuments.

**Table 4: Monuments established for the Dungeness, Washington acquisition. Coordinates are on the NAD83 (2011) datum, epoch 2010.00**

Monument ID	Latitude	Longitude	Ellipsoid (meters)
DUNGENESS_01	48° 08' 38.44996"	-123° 07' 48.88825"	-12.608
DUNGENESS_02	48° 04' 37.88554"	-123° 08' 17.05818"	67.199



To correct the continuously recorded onboard measurements of the aircraft position, QSI concurrently conducted multiple static Global Navigation Satellite System (GNSS) ground surveys (1 Hz recording frequency) over each monument. During post-processing, the static GPS data were triangulated with nearby Continuously Operating Reference Stations (CORS) using the Online Positioning User Service (OPUS<sup>1</sup>) for precise positioning. Multiple independent sessions over the same monument were processed to confirm antenna height measurements and to refine position accuracy.

Monuments were established according to the national standard for geodetic control networks, as specified in the Federal Geographic Data Committee (FGDC) Geospatial Positioning Accuracy Standards for geodetic networks.<sup>2</sup> This standard provides guidelines for classification of monument quality at the 95% confidence interval as a basis for comparing the quality of one control network to another. The monument rating for this project is shown in Table 5.

**Table 5: Federal Geographic Data Committee monument rating for network accuracy**

Direction	Rating
1.96 * St Dev <sub>NE</sub> :	0.020 m
1.96 * St Dev <sub>z</sub> :	0.020 m

For the Dungeness, Washington LiDAR project, the monument coordinates contributed no more than 2.8 cm of positional error to the geolocation of the final ground survey points and LiDAR, with 95% confidence.

## Ground Survey Points (GSPs)

Ground survey points were collected using real time kinematic, post-processed kinematic (PPK survey techniques. A Trimble R7 base unit was positioned at a nearby monument to broadcast a kinematic correction to a roving Trimble R8 GNSS receiver. All GSP measurements were made during periods with a Position Dilution of Precision (PDOP) of  $\leq 3.0$  with at least six satellites in view of the stationary and roving receivers. When collecting RTK and PPK data, the rover records data while stationary for five seconds, then calculates the pseudorange position using at least three one-second epochs. Relative errors for any GSP position must be less than 1.5 cm horizontal and 2.0 cm vertical in order to be accepted. See Table 6 for Trimble unit specifications.

GSPs were collected in areas where good satellite visibility was achieved on paved roads and other hard surfaces such as gravel or packed dirt roads. GSP measurements were not taken on highly reflective surfaces such as center line stripes or lane markings on roads due to the increased noise seen in the laser returns over these surfaces. GSPs were collected within as many flightlines as possible; however the distribution of GSPs depended on ground access constraints and monument locations and may not be equitably distributed throughout the study area (Figure 5).

<sup>1</sup> OPUS is a free service provided by the National Geodetic Survey to process corrected monument positions. <http://www.ngs.noaa.gov/OPUS>.

<sup>2</sup> Federal Geographic Data Committee, Geospatial Positioning Accuracy Standards (FGDC-STD-007.2-1998). Part 2: Standards for Geodetic Networks, Table 2.1, page 2-3. <http://www.fgdc.gov/standards/projects/FGDC-standards-projects/accuracy/part2/chapter2>

**Table 6: Trimble equipment identification**

Receiver Model	Antenna	OPUS Antenna ID	Use
Trimble R7 GNSS	Zephyr GNSS Geodetic Model 2 RoHS	TRM57971.00	Static
Trimble R8	Integrated Antenna R8 Model 2	TRM_R8_GNSS	Rover



**Top image:** QSI ground survey equipment set up over monument DUNGENESS\_01.



**Bottom image:** QSI ground surveying equipment collecting submerged bathymetric check point data.



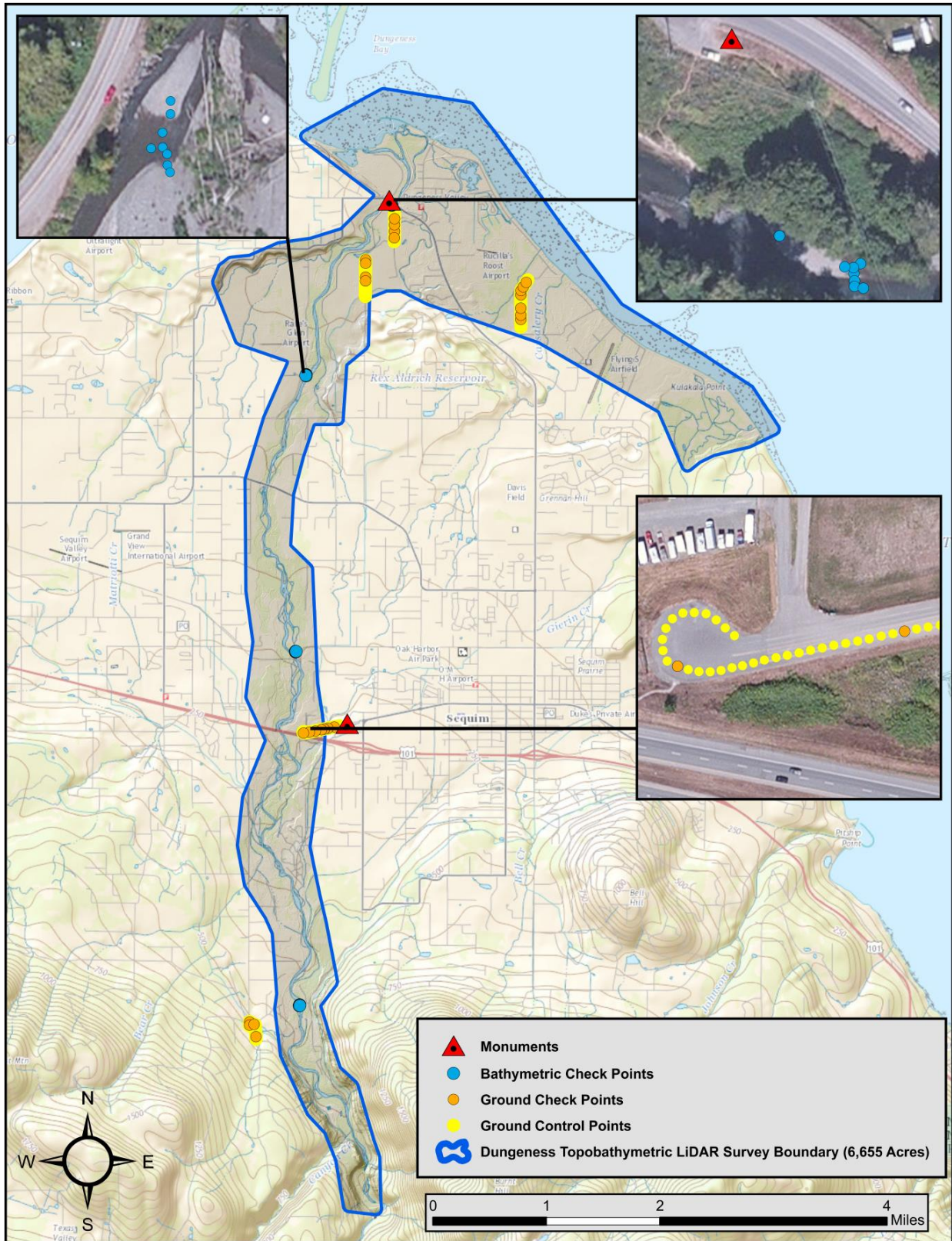
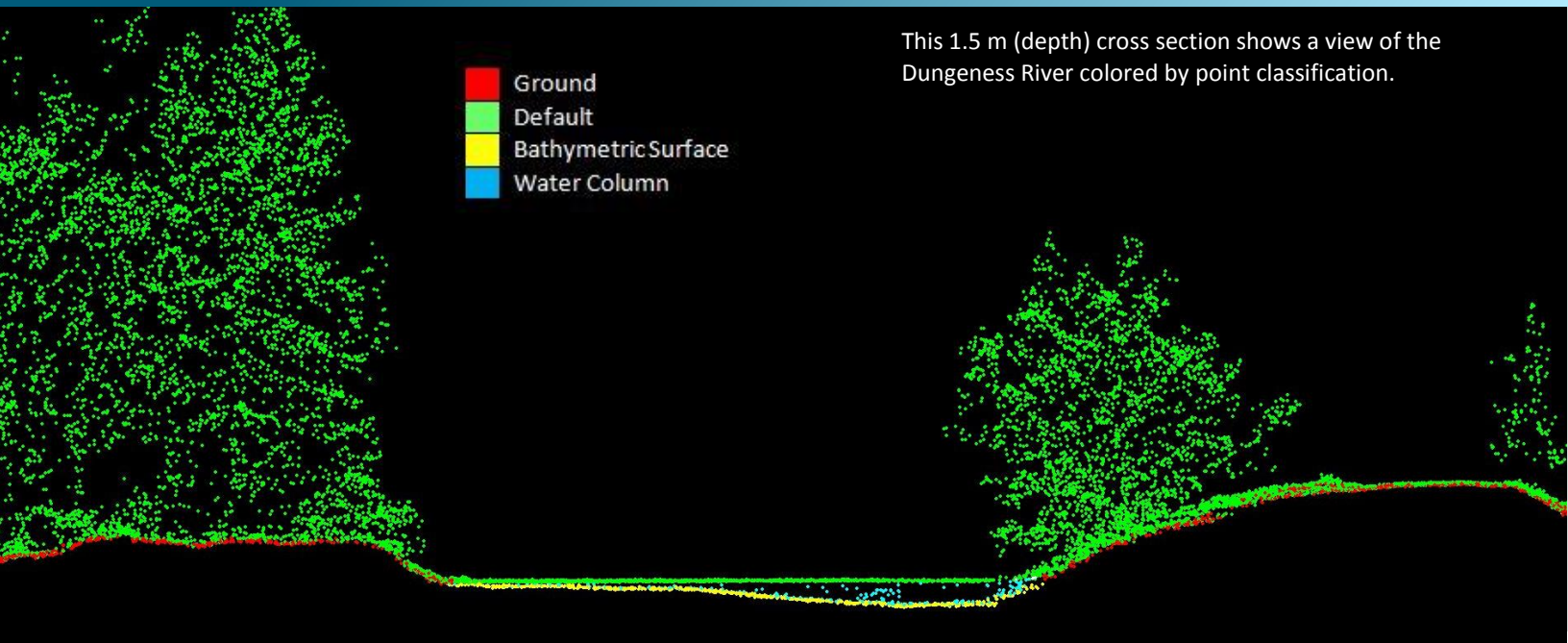


Figure 5: Dungeness, Washington Ground Survey Location Map

## PROCESSING



## Topobathymetric LiDAR Data

Upon completion of data acquisition, QSI processing staff initiated a suite of automated and manual techniques to process the data into the requested deliverables. Processing tasks included GPS control computations, smoothed best estimate trajectory (SBET) calculations, kinematic corrections, calculation of laser point position, sensor and data calibration for optimal relative and absolute accuracy, and LiDAR point classification (Table 7).

Once bathymetric points were differentiated, they were spatially corrected for refraction through the water column based on the angle of incidence of the laser. QSI refracted water column points using QSI's proprietary LAS processing software, LAS Monkey. The resulting point cloud data were classified using both manual and automated techniques. Processing methodologies were tailored for the landscape. Processing methodologies were tailored for the landscape. Brief descriptions of these tasks are shown in Table 8.

**Table 7: ASPRS LAS classification standards applied to the Dungeness, Washington dataset**

Classification Number	Classification Name	Classification Description
1	Default/Unclassified	Laser returns that are not included in the ground class, composed of vegetation and anthropogenic features
2	Ground	Laser returns that are determined to be ground using automated and manual cleaning algorithms
9	Water	NIR Laser returns that are determined to be water using automated and manual cleaning algorithms



Classification Number	Classification Name	Classification Description
25	Water Column	Refracted Riegl sensor returns that are determined to be water using automated and manual cleaning algorithms.
26	Bathymetric Bottom	Refracted Riegl sensor returns that fall within the water's edge breakline which characterize the submerged topography.
27	Water Surface	Green Laser returns that are determined to be water using automated and manual cleaning algorithms

**Table 8: LiDAR processing workflow**

LiDAR Processing Step	Software Used
Resolve kinematic corrections for aircraft position data using kinematic aircraft GPS and static ground GPS data. Develop a smoothed best estimate of trajectory (SBET) file that blends post-processed aircraft position with sensor head position and attitude recorded throughout the survey.	Waypoint Inertial Explorer v.8.6 POSPac MMS v.8.0
Calculate laser point position by associating SBET position to each laser point return time, scan angle, intensity, etc. Create raw laser point cloud data for the entire survey in *.las (ASPRS v. 1.2) format. Convert data to orthometric elevations by applying a geoid correction.	RiProcess v1.8.2 Waypoint Inertial Explorer v.8.6 Leica Cloudpro v. 1.2.2 Las Monkey 2.2.5 (QSI proprietary software)
Import raw laser points into manageable blocks (less than 500 MB) to perform manual relative accuracy calibration and filter erroneous points. Classify ground points for individual flight lines.	TerraScan v.16
Using ground classified points per each flight line, test the relative accuracy. Perform automated line-to-line calibrations for system attitude parameters (pitch, roll, heading), mirror flex (scale) and GPS/IMU drift. Calculate calibrations on ground classified points from paired flight lines and apply results to all points in a flight line. Use every flight line for relative accuracy calibration.	TerraMatch v.16
Apply refraction correction to all subsurface returns.	Las Monkey 2.2.5 (QSI proprietary software)
Classify resulting data to ground and other client designated ASPRS classifications (Table 7). Assess statistical absolute accuracy via direct comparisons of ground classified points to ground control survey data.	TerraScan v.16
Generate bare earth models as triangulated surfaces. Generate highest hit models as a surface expression of all classified points. Export all surface models as ESRI GRIDs at a 3.0 foot pixel resolution.	TerraScan v.16 TerraModeler v.16 ArcMap v. 10.2.2
Export intensity images as GeoTIFFs at a 1.5 foot pixel resolution.	ArcMap v. 10.2.2 Las Product Creator 1.5 (QSI proprietary software)

## Bathymetric Refraction

The water surface model used for refraction was generated using NIR points within the breaklines defining the water's edge. Points were filtered and edited to obtain the most accurate representation of the water surface and were used to create a water surface model TIN. A tin model is preferable to a raster based water surface model to obtain the most accurate angle of incidence during refraction. The refraction processing was done using Las Monkey; QSI's proprietary LiDAR processing tool. After refraction, the points were compared against bathymetric check points to assess accuracy.

## LiDAR Derived Products

Because hydrographic laser scanners penetrate the water surface to map submerged topography, this affects how the data should be processed and presented in derived products from the LiDAR point cloud. The following discusses certain derived products that vary from the traditional (NIR) specification and delivery format.

### Topobathymetric DEMs

Bathymetric bottom returns can be limited by depth, water clarity, and bottom surface reflectivity. Water clarity and turbidity affects the depth penetration capability of the green wavelength laser with returning laser energy diminishing by scattering throughout the water column. Additionally, the bottom surface must be reflective enough to return remaining laser energy back to the sensor at a detectable level. It is not unexpected to have no bathymetric bottom returns in turbid or non-reflective areas.

As a result, creating digital elevation models (DEMs) presents a challenge with respect to interpolation of areas with no returns. In traditional DEM creation, areas lacking ground returns are interpolated from neighboring ground returns (or breaklines in the case of hydro-flattening), with the assumption that the interpolation is close to reality. In bathymetric modeling, these assumptions are prone to error because a lack of bathymetric returns can indicate a change in elevation that the laser can no longer map due to increased depths. The resulting void areas may suggest greater depths, rather than similar elevations from neighboring bathymetric bottom returns. Therefore, QSI created a water polygon with bathymetric coverage to delineate areas with successfully mapped bathymetry. This shapefile was used to control the extent of the delivered clipped topobathymetric model to avoid false triangulation (interpolation from TIN'ing) across areas in the water with no bathymetric returns.

## Intensity Images

The difference in emitted wavelengths of the NIR (1064 nm) and Green (532 nm) lasers results in variation of the intensity information returned to the sensor for each laser. In traditional NIR LiDAR, intensity images are often made using first return information. For bathymetric LiDAR however, it is most often the last returns that capture features of interest below the water's surface. Additionally, the near-infrared wavelength is subject to spectral absorption by water, which can result in no returns over water surfaces. Due to these factors, QSI created one set of intensity images from NIR laser first returns, and one set of intensity images from green laser terrestrial first returns and all bathymetric bottom returns in order to provide the most useful intensity information. The difference in intensity images is displayed in Figure 6.

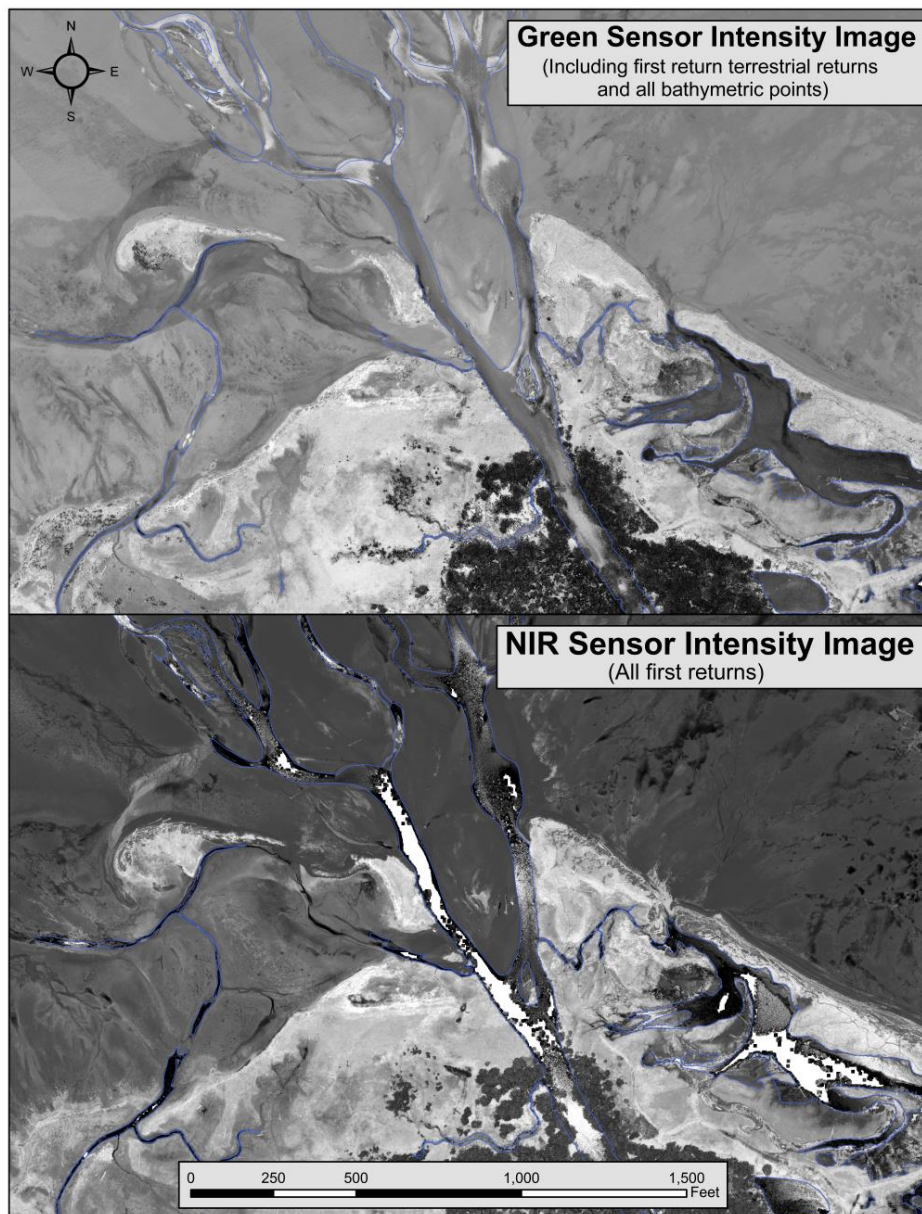


**Figure 6: A comparison of Intensity Images from Green and NIR returns in the Dungeness, Washington area**



### Bathymetric LiDAR

An underlying principle for collecting hydrographic LiDAR data is to survey near-shore areas that can be difficult to collect with other methods, such as multi-beam sonar, particularly over large areas. In order to determine the capability and effectiveness of the bathymetric LiDAR, QSI considered bathymetric bottom return density and spatial accuracy.

#### Mapped Bathymetry

To assist in evaluating performance results of the sensor, a polygon layer was created to delineate areas where bathymetry was successfully mapped. This shapefile was used to control the extent of the delivered clipped topobathymetric model and to avoid false triangulation across areas in the water with no returns. Insufficiently mapped areas were identified by triangulating bathymetric bottom points with an edge length maximum of 15.2 feet. This ensured all areas of no returns ( $> 100 \text{ ft}^2$ ), were identified as data voids. In total, 84.76% of the bathymetry in the study area was successfully mapped.



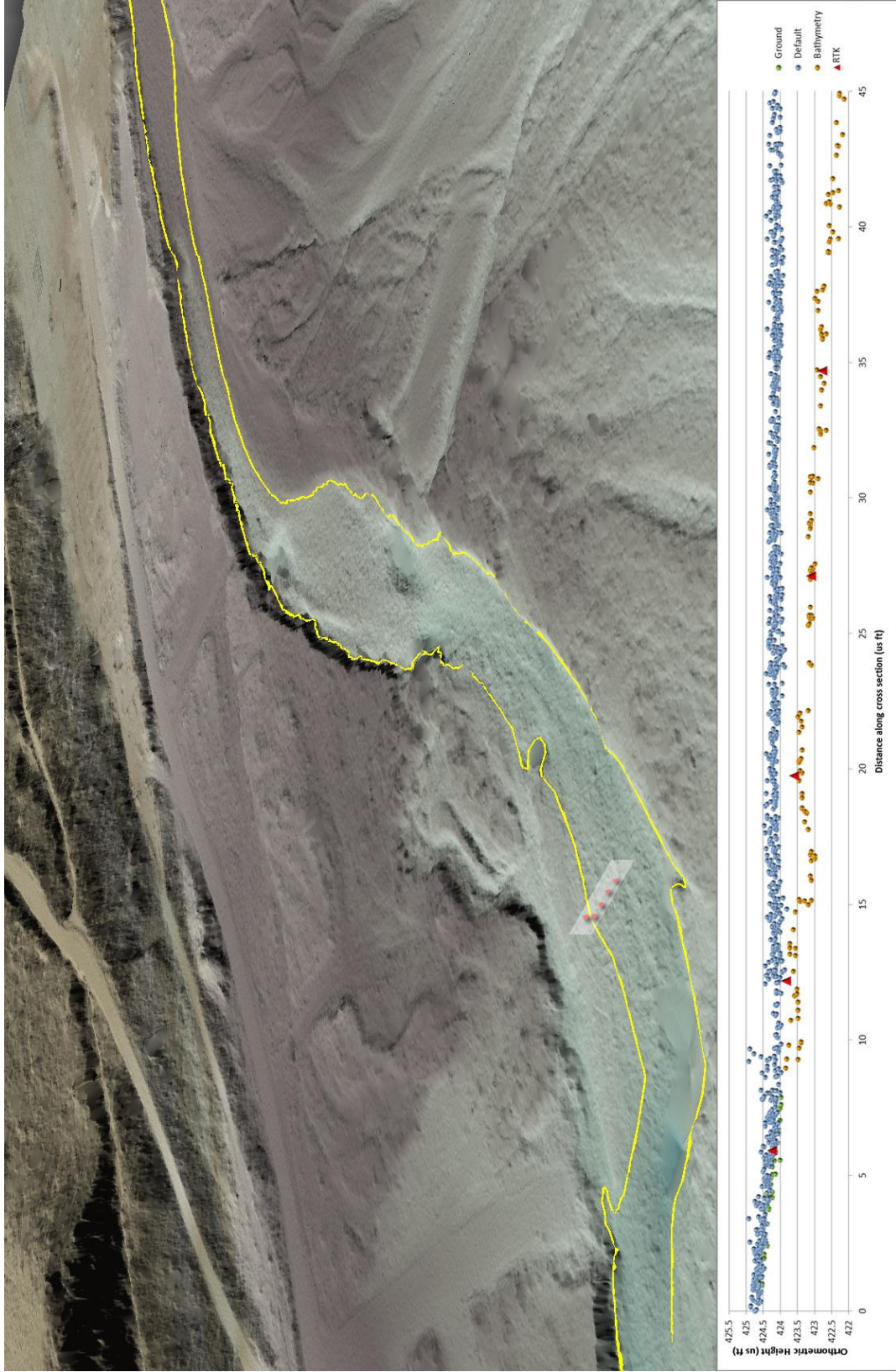


**Figure 7: This view of the Dungeness River shows the congruency between the bathymetric LIDAR survey and the collected bathymetric check point data**

# LiDAR Point Density

## First Return Point Density

The acquisition parameters were designed to acquire an average first-return density of 4 points/m<sup>2</sup> (0.37 points/ft<sup>2</sup>) for the topobathymetric AOI, and 6 points/ m<sup>2</sup> (0.56 points/ft<sup>2</sup>) for the NIR AOI. First return density describes the density of pulses emitted from the laser that return at least one echo to the system. Multiple returns from a single pulse were not considered in first return density analysis. Some types of surfaces (e.g., breaks in terrain, water and steep slopes) may have returned fewer pulses than originally emitted by the laser.

First returns typically reflect off the highest feature on the landscape within the footprint of the pulse. In forested or urban areas the highest feature could be a tree, building or power line, while in areas of unobstructed ground, the first return will be the only echo and represents the bare earth surface.

The average first-return point density value of the green wavelength LiDAR data for the Dungeness, Washington project was 1.35 points/ft<sup>2</sup> (14.50 points/m<sup>2</sup>) while the average first-return point density value of the NIR wavelength LiDAR data was 5.80 points/ft<sup>2</sup> (62.39 points/m<sup>2</sup>) (Table 9). The cumulative average first return point density value was 7.14 points/ft<sup>2</sup> (76.89 points/m<sup>2</sup>). The statistical and spatial distributions of all first return densities per 100 m x 100 m cell are portrayed in Figure 8 through Figure 13.

**Table 9: Average First Return LiDAR point densities**

First Return Type	Point Density
<b>NIR &amp; Green Cumulative First Returns</b>	7.14 points/ft <sup>2</sup>
	76.89 points/m <sup>2</sup>
<b>NIR Sensor First Returns</b>	5.80 points/ft <sup>2</sup>
	62.39 points/m <sup>2</sup>
<b>Green Sensor First Returns</b>	1.35 points/ft <sup>2</sup>
	14.50 points/m <sup>2</sup>

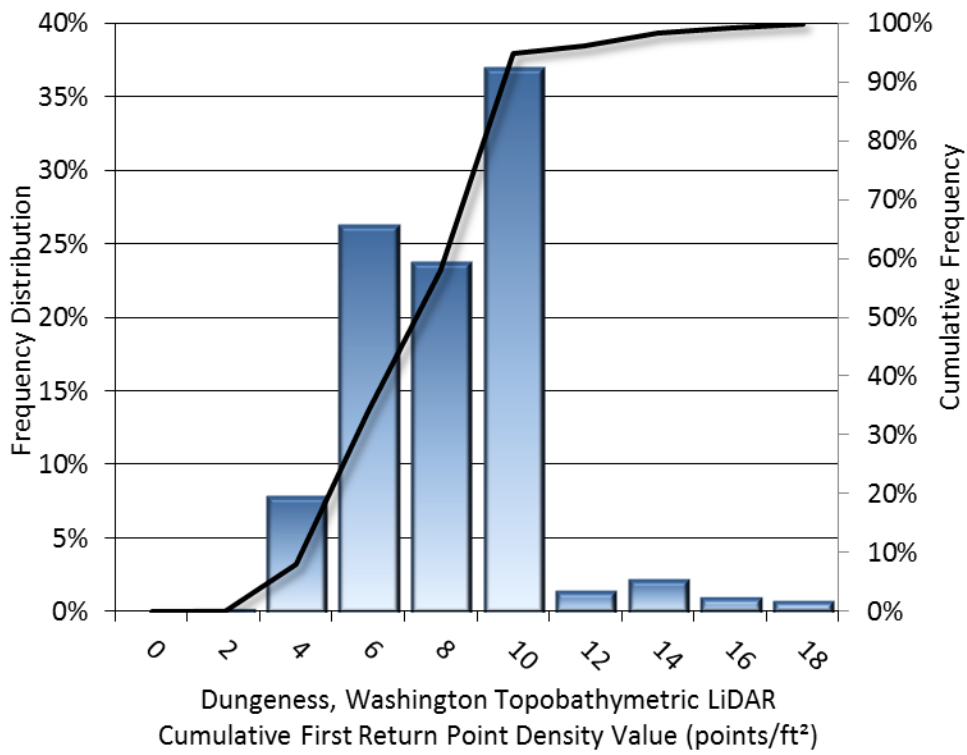


**Figure 8: Frequency distribution of cumulative first return densities per 100 x 100 m cell**

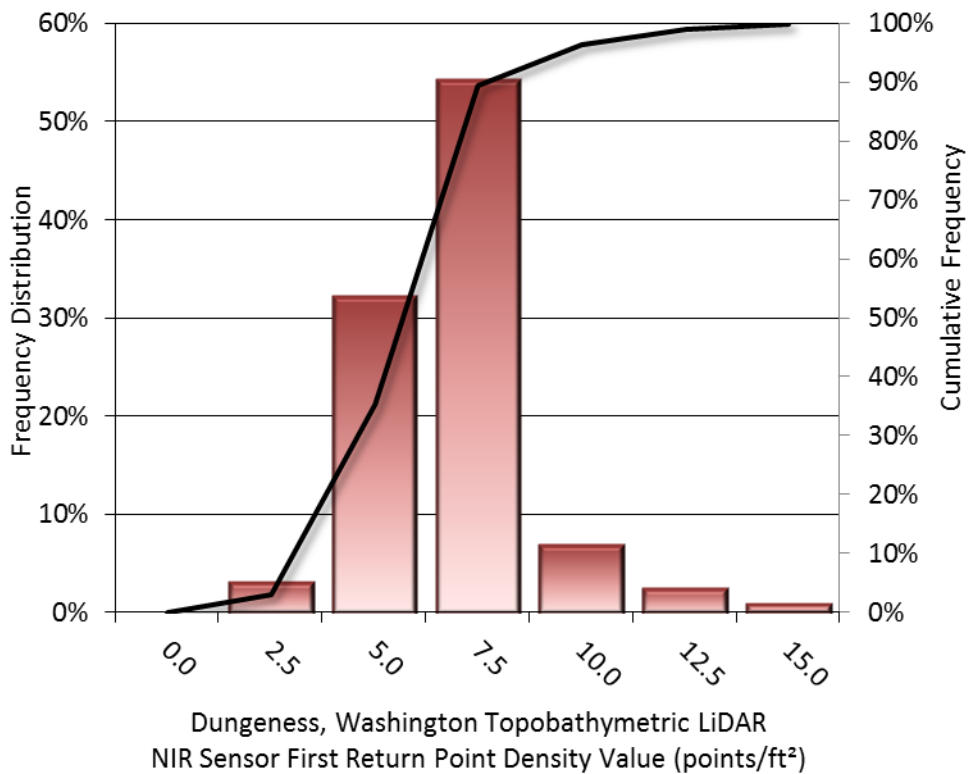


**Figure 9: Frequency distribution of NIR sensor first return densities per 100 x 100 m cell**



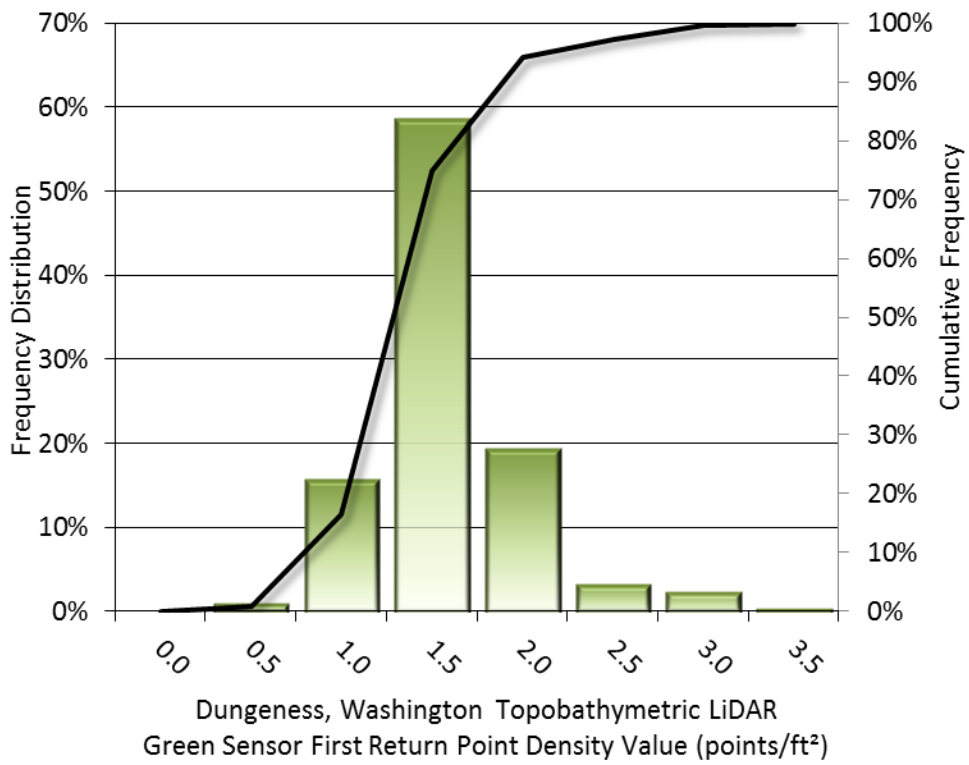


**Figure 10: Frequency distribution of green sensor first return densities per 100 x 100 m cell**

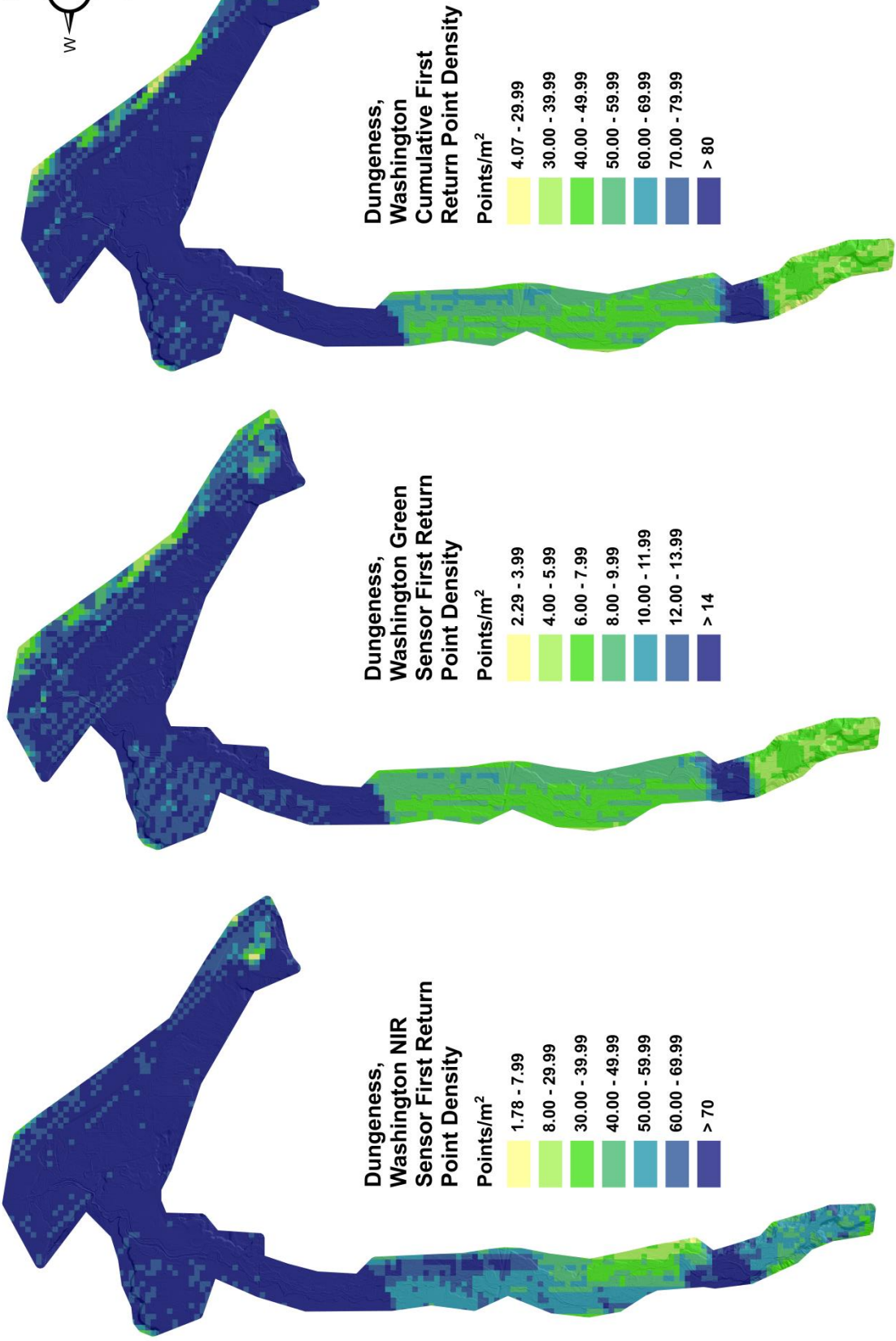
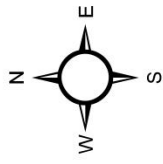


Figure 11: First return density maps for the Dungeness, Washington site (100 m x 100 m cells)

## Bathymetric and Ground Classified Point Densities

The density of ground classified LiDAR returns and bathymetric bottom returns were also analyzed for this project. Terrain character, land cover, and ground surface reflectivity all influenced the density of ground surface returns. In vegetated areas, fewer pulses may have penetrated the canopy, resulting in lower ground density. Similarly, the density of bathymetric bottom returns was influenced by turbidity, depth, and bottom surface reflectivity. In turbid areas, fewer pulses may have penetrated the water surface, resulting in lower bathymetric density.

The ground and bathymetric bottom classified density of LiDAR data for the Dungeness, Washington project was 1.24 points/ft<sup>2</sup> (13.39 points/m<sup>2</sup>) (Table 10). The statistical and spatial distributions ground classified and bathymetric bottom return densities per 100 m x 100 m cell are portrayed in Figure 13 and Figure 13.

Additionally, for the Dungeness, Washington project, density values of only bathymetric bottom returns were calculated for areas considered successfully mapped by the bathymetric coverage polygon. Within the successfully mapped area, a bathymetric bottom return density of 0.73 points/ft<sup>2</sup> (7.95 points/m<sup>2</sup>) was achieved.

**Table 10: Average Ground and Bathymetric Classified LiDAR point densities**

Classification	Point Density
Ground and Bathymetric Bottom Classified Returns	1.24 points/ft <sup>2</sup> 13.39 points/m <sup>2</sup>

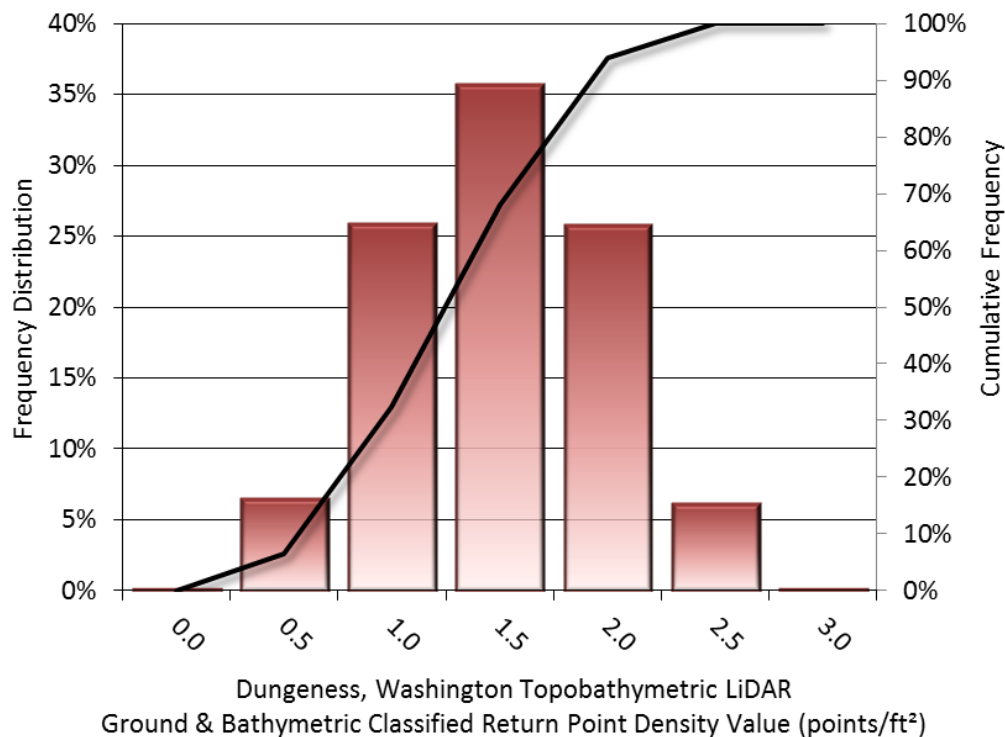


**Figure 12: Frequency distribution of ground and bathymetric bottom classified point density values per 100 x 100 m cell**



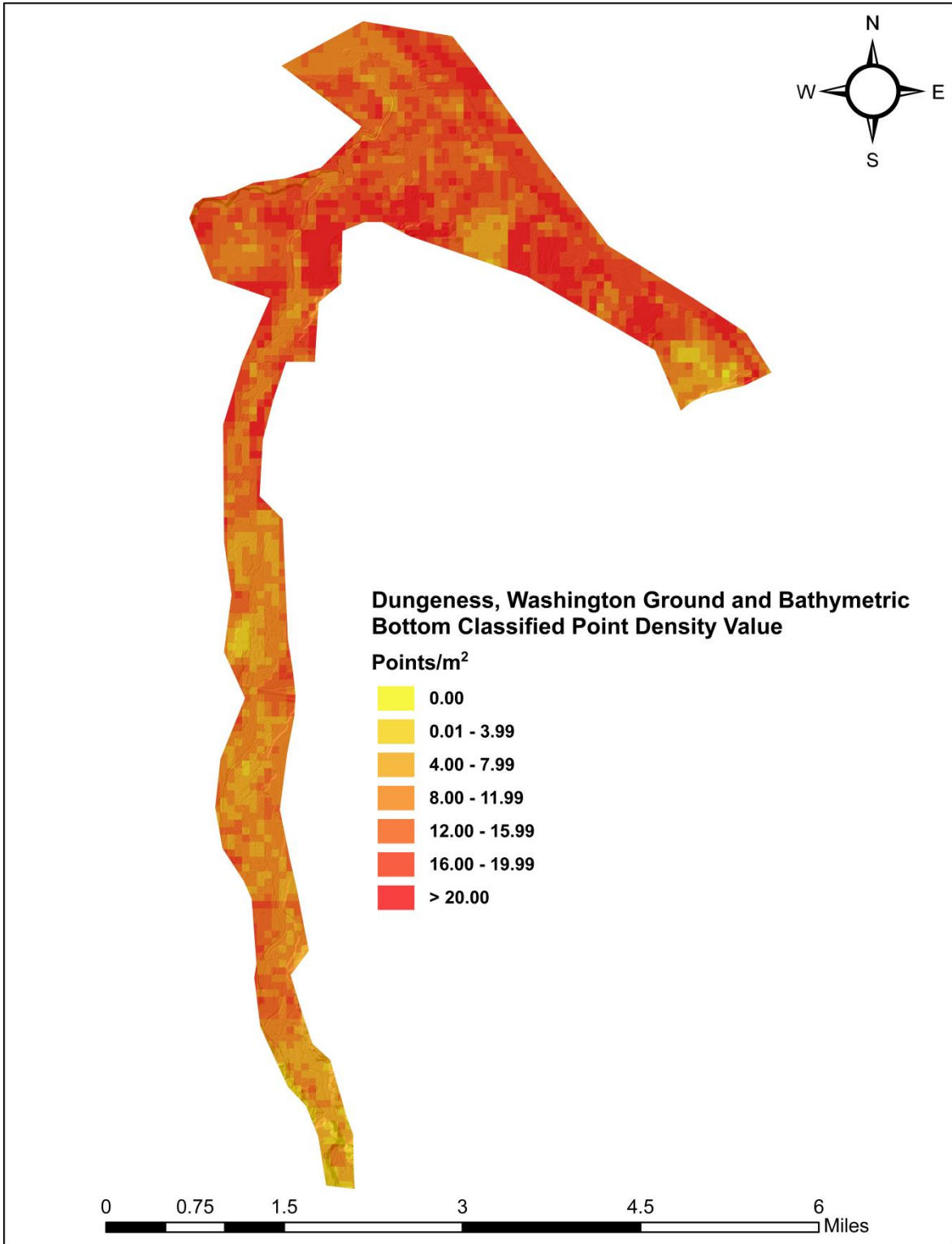


**Figure 13: Ground density map for the Dungeness, Washington site (100 m x 100 m cells)**

## LiDAR Accuracy Assessments

The accuracy of the LiDAR data collection can be described in terms of absolute accuracy (the consistency of the data with external data sources) and relative accuracy (the consistency of the dataset with itself). See Appendix A for further information on sources of error and operational measures used to improve relative accuracy.

### LiDAR Absolute Accuracy

Absolute accuracy was assessed using Non-vegetated Vertical Accuracy (NVA) reporting designed to meet guidelines presented in the FGDC National Standard for Spatial Data Accuracy<sup>3</sup>. NVA compares known ground quality assurance point data collected on open, bare earth surfaces with level slope (<20°) to the triangulated surface generated by the LiDAR points. NVA is a measure of the accuracy of LiDAR point data in open areas where the LiDAR system has a high probability of measuring the ground surface and is evaluated at the 95% confidence interval ( $1.96 * RMSE$ ), as shown in Table 11.

The mean and standard deviation (sigma  $\sigma$ ) of divergence of the ground surface model from ground check point coordinates are also considered during accuracy assessment. These statistics assume the error for x, y and z is normally distributed, and therefore the skew and kurtosis of distributions are also considered when evaluating error statistics. For the Dungeness, Washington survey, 26 ground check points were withheld in total resulting in a non-vegetated vertical accuracy of 0.136 feet (0.041 meters) (Figure 14).

Additionally, bathymetric check points (submerged or along the water's edge) were collected in order to assess the vertical accuracy of the submerged surface (bathymetry of Platte River). Evaluation of 32 bathymetric check points at the 95% confidence level resulted in a value of 0.187 feet (0.057 meters) (Table 11, Figure 15).

QSI also assessed absolute accuracy using 482 ground control points. Although these points were used in the calibration and post-processing of the LiDAR point cloud, they may still provide a good indication of the overall accuracy of the LiDAR dataset, and therefore have been provided in Table 11 and Figure 15.

---

<sup>3</sup> Federal Geographic Data Committee, ASPRS POSITIONAL ACCURACY STANDARDS FOR DIGITAL GEOSPATIAL DATA EDITION 1, Version 1.0, NOVEMBER 2014. <http://www.asprs.org/PAD-Division/ASPRS-POSITIONAL-ACCURACY-STANDARDS-FOR-DIGITAL-GEOSPATIAL-DATA.html>.

**Table 11: Absolute accuracy results**

Absolute Accuracy			
	Ground Check Points	Bathymetric Check Points	Ground Control Points
Sample	26 points	32 points	482 points
NVA (1.96*RMSE)	0.136 ft	0.187 ft	0.098 ft
	0.041 m	0.057 m	0.030 m
Average	-0.023 ft	-0.061 ft	-0.009 ft
	-0.007 m	-0.019 m	-0.003 m
Median	-0.008 ft	-0.079 ft	-0.007 ft
	-0.003 m	-0.024 m	-0.002 m
RMSE	0.069 ft	0.095 ft	0.050 ft
	0.021 m	0.029 m	0.015 m
Standard Deviation (1σ)	0.067 ft	0.074 ft	0.049 ft
	0.020 m	0.023 m	0.015 m

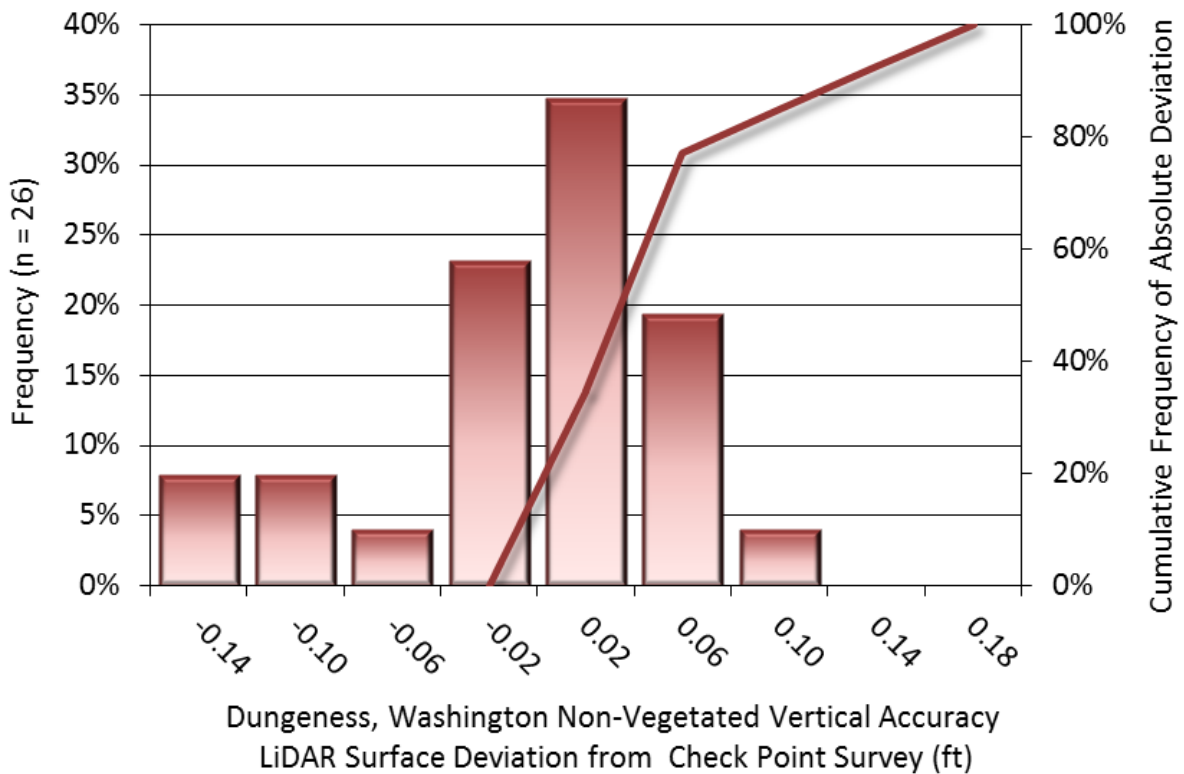


**Figure 14: Frequency histogram for LiDAR surface deviation from ground check point values**



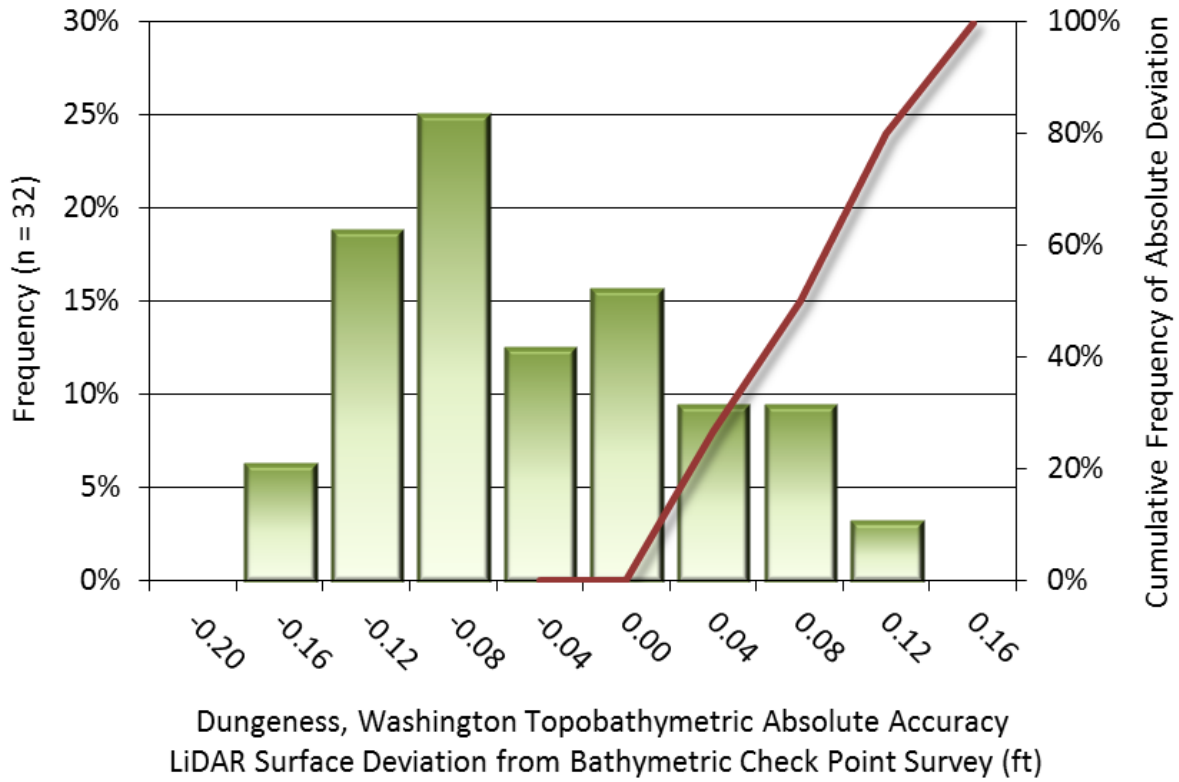


Figure 15: Frequency histogram for LiDAR surface deviation from bathymetric check point values

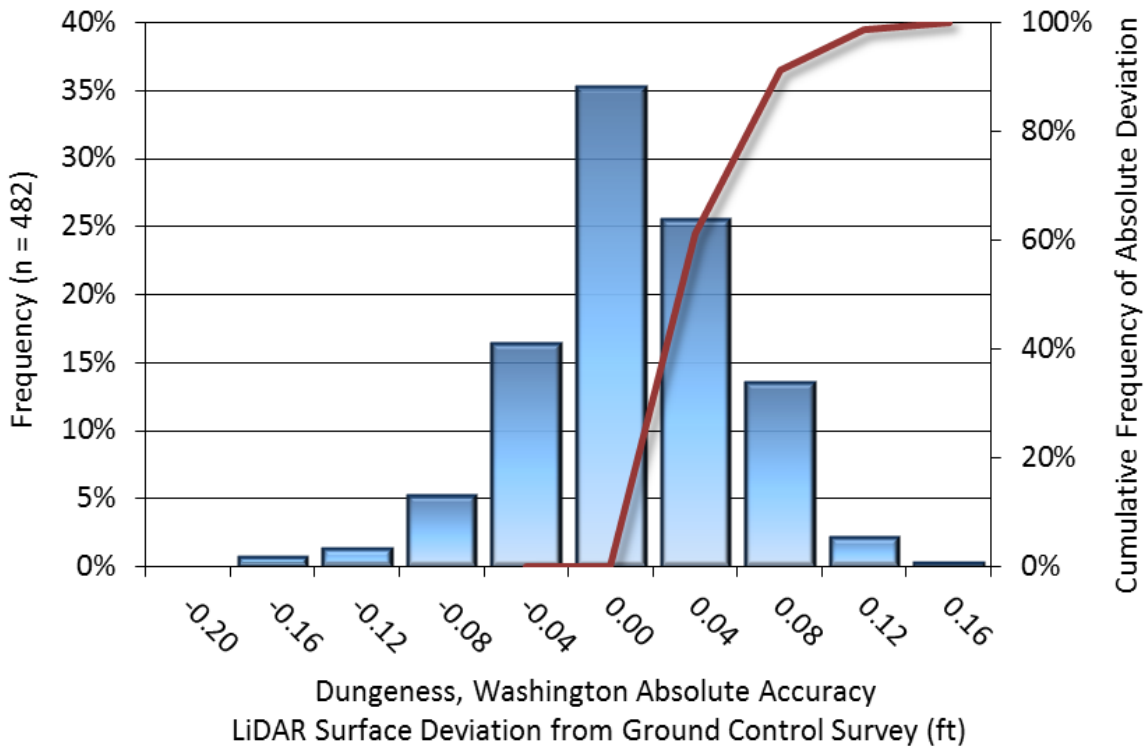


Figure 16: Frequency histogram for LiDAR surface deviation from ground control point values

## LiDAR Relative Vertical Accuracy

Relative vertical accuracy refers to the internal consistency of the data set as a whole: the ability to place an object in the same location given multiple flight lines, GPS conditions, and aircraft attitudes. When the LiDAR system is well calibrated, the swath-to-swath vertical divergence is low (<0.10 meters). The relative vertical accuracy was computed by comparing the ground surface model of each individual flight line with its neighbors in overlapping regions. The average (mean) line to line relative vertical accuracy of NIR flightlines for the Dungeness, Washington LiDAR project was 0.073 feet (0.022 meters), while the average relative accuracy of Green flightlines for the Dungeness, Washington LiDAR project was 0.088 feet (0.027 meters). Overall, the Dungeness topobathymetric LiDAR survey resulted in a cumulative relative vertical accuracy of 0.078 feet (0.024 meters). Detailed results are provided in Table 12 and Figure 17 through Figure 19.

**Table 12: Relative accuracy results**

Relative Accuracy			
	Cumulative Results (all flightlines)	NIR Laser Flightlines	Green Laser Flightlines
<b>Sample</b>	123 surfaces	62 surfaces	61 surfaces
<b>Average</b>	0.078 ft 0.024 m	0.073 ft 0.022 m	0.088 ft 0.027 m
<b>Median</b>	0.074 ft 0.023 m	0.071 ft 0.022 m	0.082 ft 0.025 m
<b>RMSE</b>	0.084 ft 0.026 m	0.076 ft 0.023 m	0.092 ft 0.028 m
<b>Standard Deviation (1σ)</b>	0.022 ft 0.007 m	0.014 ft 0.004 m	0.027 ft 0.008 m
<b>1.96σ</b>	0.044 ft 0.013 m	0.027 ft 0.008 m	0.053 ft 0.016 m

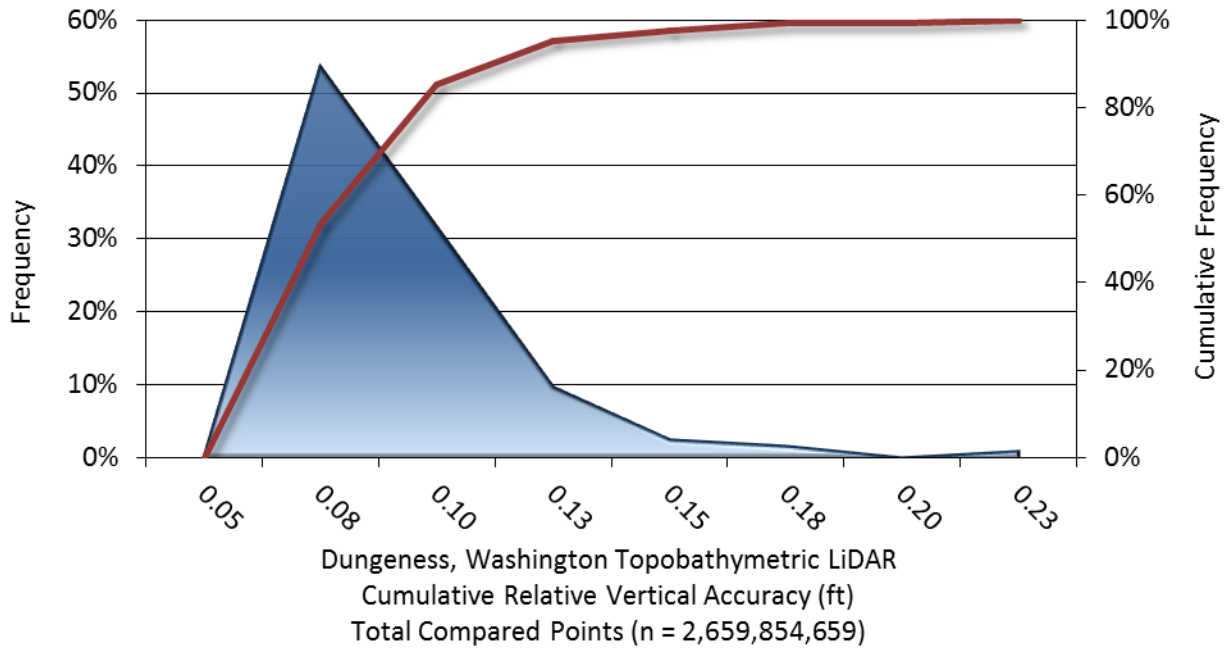


**Figure 17: Frequency plot for relative vertical accuracy between integrated flight lines**

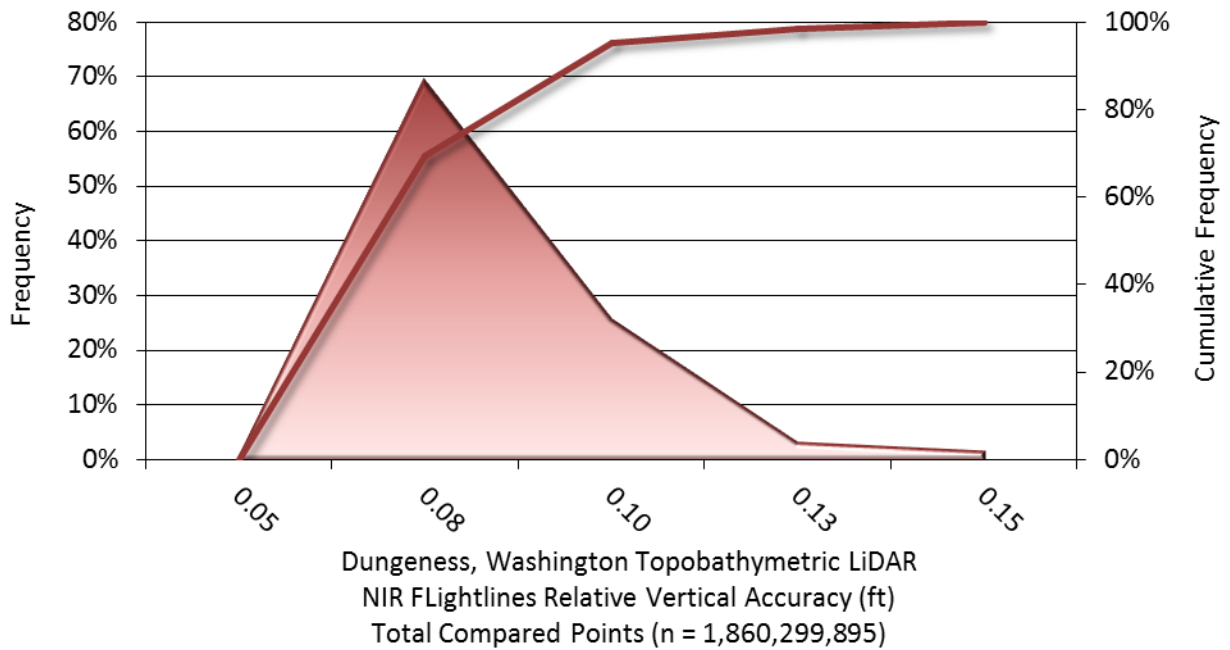


**Figure 18: Frequency plot for relative vertical accuracy between NIR flight lines**



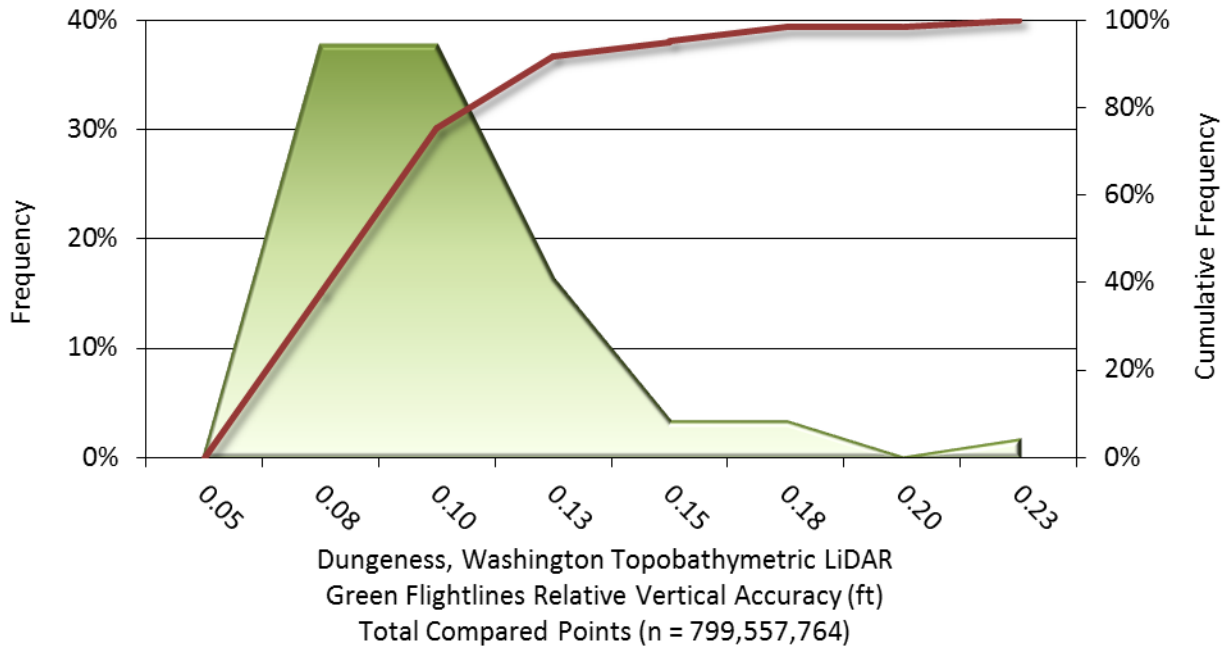


**Figure 19: Frequency plot for relative vertical accuracy between Green flight lines**

## CERTIFICATIONS

Quantum Spatial, Inc. provided LiDAR services for the Dungeness, Washington project as described in this report.

I, Tucker Selko, have reviewed the attached report for completeness and hereby state that it is a complete and accurate report of this project.

Tucker Selko  
Tucker Selko (Mar 14, 2017)

Mar 14, 2017

---

Tucker Selko  
Project Manager  
Quantum Spatial, Inc.

I, Evon P. Silvia, PLS, being duly registered as a Professional Land Surveyor in and by the state of Washington, hereby certify that the methodologies, static GNSS occupations used during airborne flights, and ground survey point collection were performed using commonly accepted Standard Practices. Field work conducted for this report was conducted between December 13 and 16, 2016.

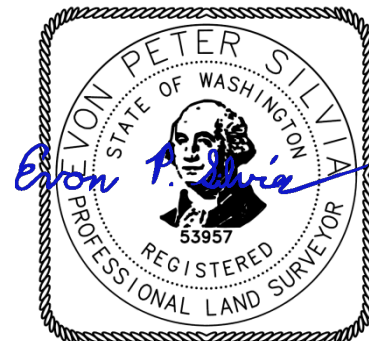
Accuracy statistics shown in the Accuracy Section of this Report have been reviewed by me and found to meet the “National Standard for Spatial Data Accuracy”.

Evon P. Silvia

Mar 14, 2017

---

Evon P. Silvia, PLS  
Quantum Spatial, Inc.  
Corvallis, OR 97333



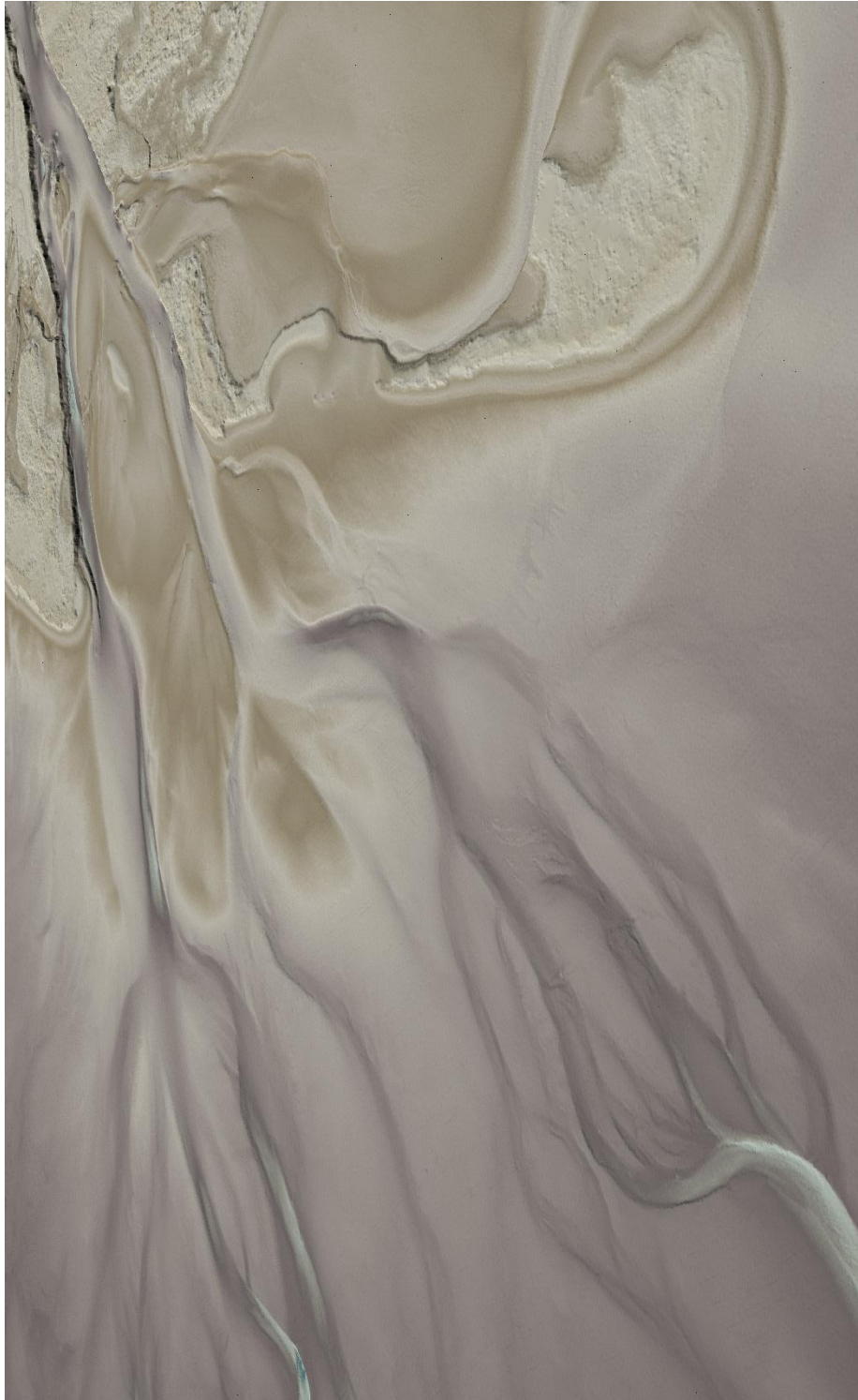
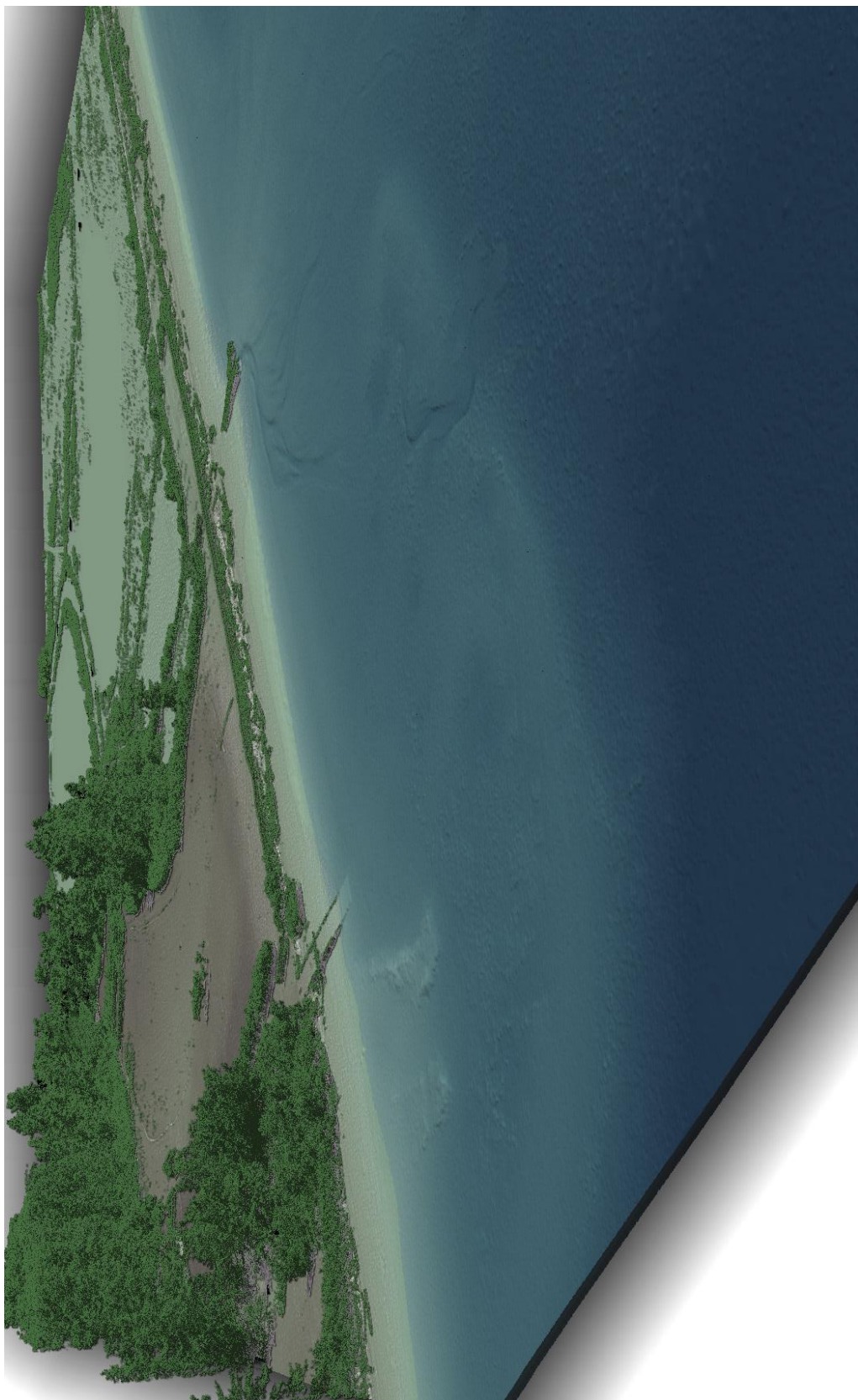


Figure 20: View of the Dungeness River meeting the Pacific Ocean. The image is created from the gridded, bare earth and bathymetric bottom LiDAR returns colored by elevation





**Figure 21: View of the mouth of the Dungeness River. The image is created from the gridded, bare earth and bathymetric bottom LiDAR returns colored by elevation, overlaid with the water's edge breaklines**



**Figure 22: View of the Sequim, Washington coastline. The image is created from the gridded, bare earth and bathymetric bottom LiDAR returns colored by elevation and above ground LiDAR point cloud.**

**1-sigma ( $\sigma$ ) Absolute Deviation:** Value for which the data are within one standard deviation (approximately 68<sup>th</sup> percentile) of a normally distributed data set.

**1.96 \* RMSE Absolute Deviation:** Value for which the data are within two standard deviations (approximately 95<sup>th</sup> percentile) of a normally distributed data set, based on the FGDC standards for Fundamental Vertical Accuracy (FVA) reporting.

**Accuracy:** The statistical comparison between known (surveyed) points and laser points. Typically measured as the standard deviation ( $\sigma$ ) and root mean square error (RMSE).

**Absolute Accuracy:** The vertical accuracy of LiDAR data is described as the mean and standard deviation ( $\sigma$ ) of divergence of LiDAR point coordinates from ground survey point coordinates. To provide a sense of the model predictive power of the dataset, the root mean square error (RMSE) for vertical accuracy is also provided. These statistics assume the error distributions for x, y and z are normally distributed, and thus we also consider the skew and kurtosis of distributions when evaluating error statistics.

**Relative Accuracy:** Relative accuracy refers to the internal consistency of the data set; i.e., the ability to place a laser point in the same location over multiple flight lines, GPS conditions and aircraft attitudes. Affected by system attitude offsets, scale and GPS/IMU drift, internal consistency is measured as the divergence between points from different flight lines within an overlapping area. Divergence is most apparent when flight lines are opposing. When the LiDAR system is well calibrated, the line-to-line divergence is low (<10 cm).

**Root Mean Square Error (RMSE):** A statistic used to approximate the difference between real-world points and the LiDAR points. It is calculated by squaring all the values, then taking the average of the squares and taking the square root of the average.

**Data Density:** A common measure of LiDAR resolution, measured as points per square meter.

**Digital Elevation Model (DEM):** File or database made from surveyed points, containing elevation points over a contiguous area. Digital terrain models (DTM) and digital surface models (DSM) are types of DEMs. DTMs consist solely of the bare earth surface (ground points), while DSMs include information about all surfaces, including vegetation and man-made structures.

**Intensity Values:** The peak power ratio of the laser return to the emitted laser, calculated as a function of surface reflectivity.

**Nadir:** A single point or locus of points on the surface of the earth directly below a sensor as it progresses along its flight line.

**Overlap:** The area shared between flight lines, typically measured in percent. 100% overlap is essential to ensure complete coverage and reduce laser shadows.

**Pulse Rate (PR):** The rate at which laser pulses are emitted from the sensor; typically measured in thousands of pulses per second (kHz).

**Pulse Returns:** For every laser pulse emitted, the number of wave forms (i.e., echos) reflected back to the sensor. Portions of the wave form that return first are the highest element in multi-tiered surfaces such as vegetation. Portions of the wave form that return last are the lowest element in multi-tiered surfaces.

**Real-Time Kinematic (RTK) Survey:** A type of surveying conducted with a GPS base station deployed over a known monument with a radio connection to a GPS rover. Both the base station and rover receive differential GPS data and the baseline correction is solved between the two. This type of ground survey is accurate to 1.5 cm or less.

**Post-Processed Kinematic (PPK) Survey:** GPS surveying is conducted with a GPS rover collecting concurrently with a GPS base station set up over a known monument. Differential corrections and precisions for the GNSS baselines are computed and applied after the fact during processing. This type of ground survey is accurate to 1.5 cm or less.

**Scan Angle:** The angle from nadir to the edge of the scan, measured in degrees. Laser point accuracy typically decreases as scan angles increase.

**Native LiDAR Density:** The number of pulses emitted by the LiDAR system, commonly expressed as pulses per square meter.



# APPENDIX A - ACCURACY CONTROLS

## Relative Accuracy Calibration Methodology:

**Manual System Calibration:** Calibration procedures for each mission require solving geometric relationships that relate measured swath-to-swath deviations to misalignments of system attitude parameters. Corrected scale, pitch, roll and heading offsets were calculated and applied to resolve misalignments. The raw divergence between lines was computed after the manual calibration was completed and reported for each survey area.

**Automated Attitude Calibration:** All data were tested and calibrated using TerraMatch automated sampling routines. Ground points were classified for each individual flight line and used for line-to-line testing. System misalignment offsets (pitch, roll and heading) and scale were solved for each individual mission and applied to respective mission datasets. The data from each mission were then blended when imported together to form the entire area of interest.

**Automated Z Calibration:** Ground points per line were used to calculate the vertical divergence between lines caused by vertical GPS drift. Automated Z calibration was the final step employed for relative accuracy calibration.

## LiDAR accuracy error sources and solutions:

Type of Error	Source	Post Processing Solution
GPS (Static/Kinematic)	Long Base Lines	None
	Poor Satellite Constellation	None
	Poor Antenna Visibility	Reduce Visibility Mask
Relative Accuracy	Poor System Calibration	Recalibrate IMU and sensor offsets/settings
	Inaccurate System	None
Laser Noise	Poor Laser Timing	None
	Poor Laser Reception	None
	Poor Laser Power	None
	Irregular Laser Shape	None

## Operational measures taken to improve relative accuracy:

**Low Flight Altitude:** Terrain following was employed to maintain a constant above ground level (AGL). Laser horizontal errors are a function of flight altitude above ground (about 1/3000<sup>th</sup> AGL flight altitude).

**Focus Laser Power at narrow beam footprint:** A laser return must be received by the system above a power threshold to accurately record a measurement. The strength of the laser return (i.e., intensity) is a function of laser emission power, laser footprint, flight altitude and the reflectivity of the target. While surface reflectivity cannot be controlled, laser power can be increased and low flight altitudes can be maintained.

**Reduced Scan Angle:** Edge-of-scan data can become inaccurate. The scan angle was reduced to a maximum of  $\pm 20^\circ$  from nadir, creating a narrow swath width and greatly reducing laser shadows from trees and buildings.

**Quality GPS:** Flights took place during optimal GPS conditions (e.g., 6 or more satellites and PDOP [Position Dilution of Precision] less than 3.0). Before each flight, the PDOP was determined for the survey day. During all flight times, a dual frequency DGPS base station recording at 1 second epochs was utilized and a maximum baseline length between the aircraft and the control points was less than 13 nm at all times.

**Ground Survey:** Ground survey point accuracy (<1.5 cm RMSE) occurs during optimal PDOP ranges and targets a minimal baseline distance of 4 miles between GPS rover and base. Robust statistics are, in part, a function of sample size (n) and distribution. Ground survey points are distributed to the extent possible throughout multiple flight lines and across the survey area.

**50% Side-Lap (100% Overlap):** Overlapping areas are optimized for relative accuracy testing. Laser shadowing is minimized to help increase target acquisition from multiple scan angles. Ideally, with a 50% side-lap, the nadir portion of one flight line coincides with the swath edge portion of overlapping flight lines. A minimum of 50% side-lap with terrain-followed acquisition prevents data gaps.

**Opposing Flight Lines:** All overlapping flight lines have opposing directions. Pitch, roll and heading errors are amplified by a factor of two relative to the adjacent flight line(s), making misalignments easier to detect and resolve.